

# The Oort cloud: shape and dynamics

Marc Fouchard (University of Lille 1 / IMCCE)

Hans Rickman (Uppsala Univ. / PAS Space Research Center, Warsaw)

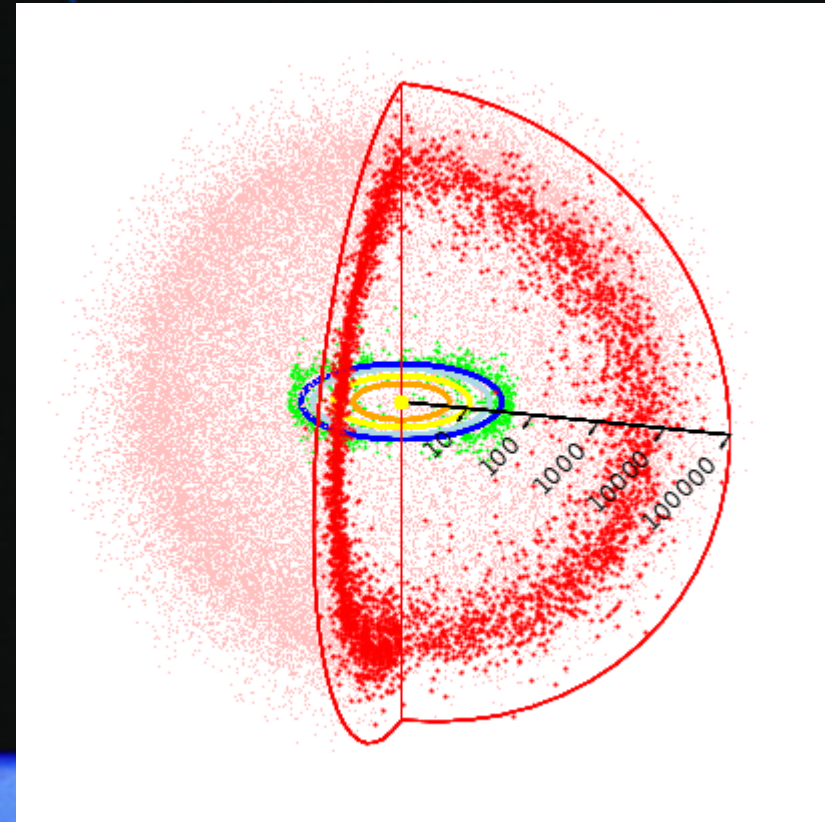
Christiane Froeschlé (OCA)

Giovanni Valsecchi (IAPS-INAF, Roma)

Workshop in honour of Hans Rickman - Meudon, May 17<sup>th</sup>-19<sup>th</sup>, 2016

# Three main perturbators

- Stellar perturbations caused by a close encounter of the Sun with a passing star ;
- Galactic tides caused by the difference of the gravitational attraction of the entire Galaxy on the Sun and on the comet ;
- Planetary perturbations, when the trajectory of the Oort cloud comets penetrate within the planetary region of the solar system ;
- The Giant Molecular cloud, usually not taken into account, even if they might be efficient perturbators of the Oort cloud.

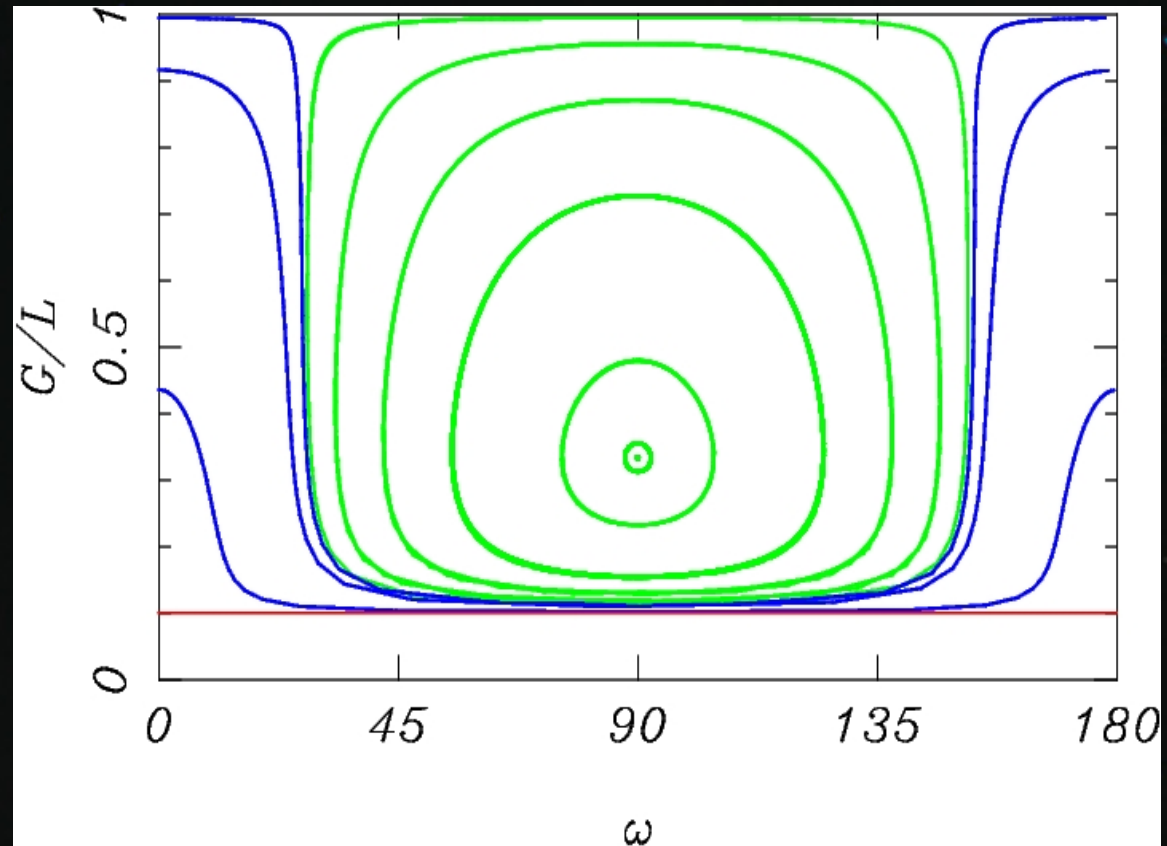


# The Galactic tides: integrable case

## ■ Constants of motion:

$$a = 30\,000 \text{ AU}$$

$$\sqrt{1 - e^2} \cos i = 0.1$$



## ■ Period and perturbations strength over one orbital period:

$$P_e \propto P_{orb}^{-1},$$

$$\Delta q \propto a^{7/2}$$



# The stellar environment of the Sun

Construction of a sample of random stellar passages with the following criteria according to the stellar type (13 different types are used):

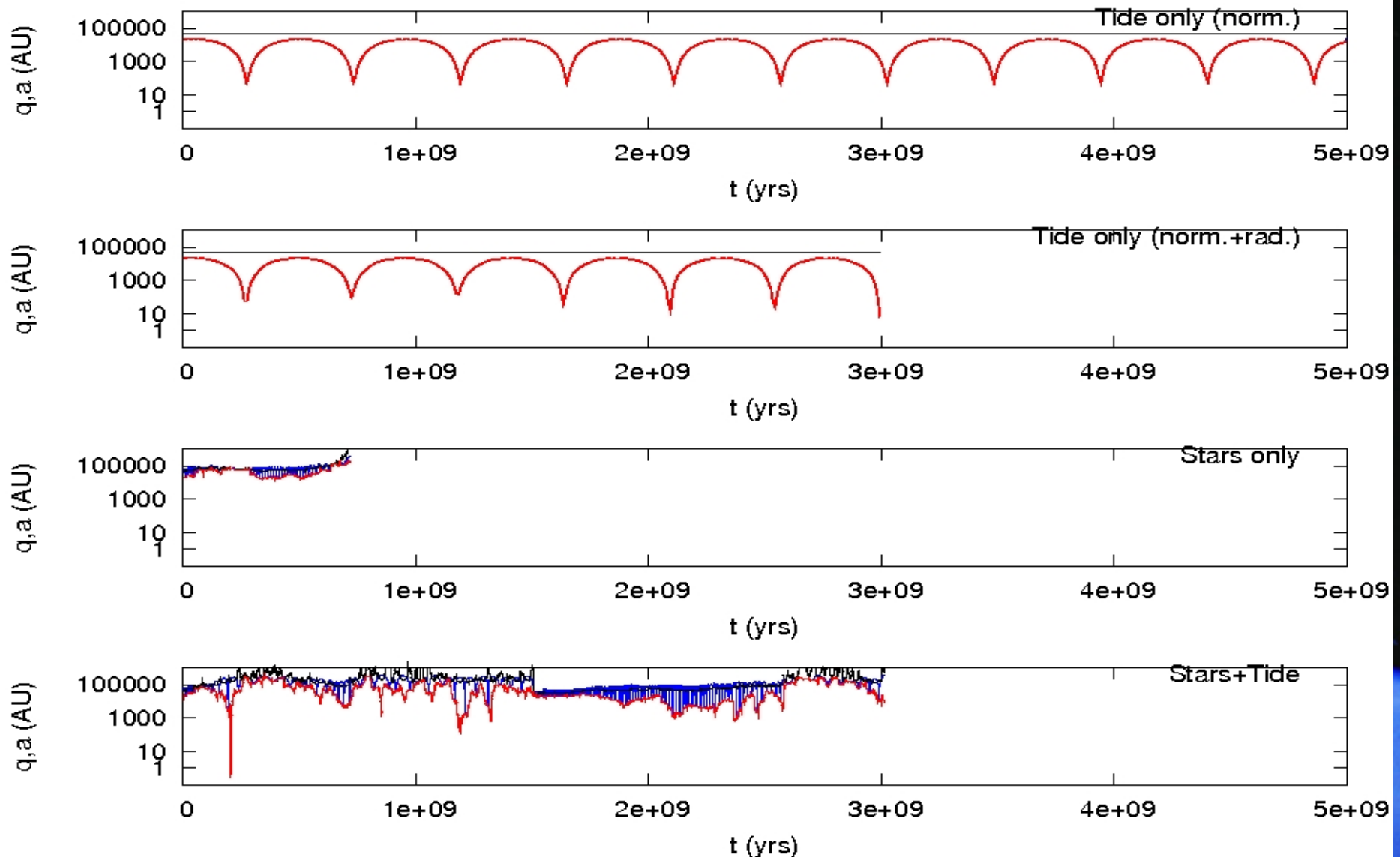
- the stellar mass is fixed;
- speed and time of perihelion passage are chosen randomly respecting the actual observed distribution;
- velocity direction is chosen randomly corresponding to an isotropic distribution.

197 906 stellar passages within 400,000 AU from the Sun in 5 Gyr are thus defined during a 5 Gyr time span with the following characteristics:

Type	Mass ( $M_{\odot}$ )	Enc. Freq.	V (km/s)	$\sigma$ (km/s)
gi	4	0.06	49.7	17.5
B0	9	0.01	24.6	6.7
A0	3.2	0.03	27.5	9.3
A5	2.1	0.04	29.3	10.4
F0	1.7	0.15	36.5	12.6
F5	1.3	0.08	43.6	15.6
G0	1.1	0.22	49.8	17.1
G5	0.93	0.35	49.6	17.9
K0	0.78	0.34	42.6	15
K5	0.69	0.85	54.3	19.2
M0	0.47	1.29	50	18
M5	0.21	6.39	51.8	18.3
wd	0.9	0.72	80.2	28.2

# Example I

—  $a$  —  $q$  —  $r$



# The Tidal Active Zone

$t = 0$

**The Oort cloud**

$q_{\min} > 5 \text{ A.U.}$

**T.A.Z.**  
 $q_{\min} < 5 \text{ A.U.}$

$t > 0$

**The Oort cloud**

$q_{\min} > 5 \text{ A.U.}$

**T.A.Z.**  
 $q_{\min} < 5 \text{ A.U.}$

**Tide action**

**Observable region**

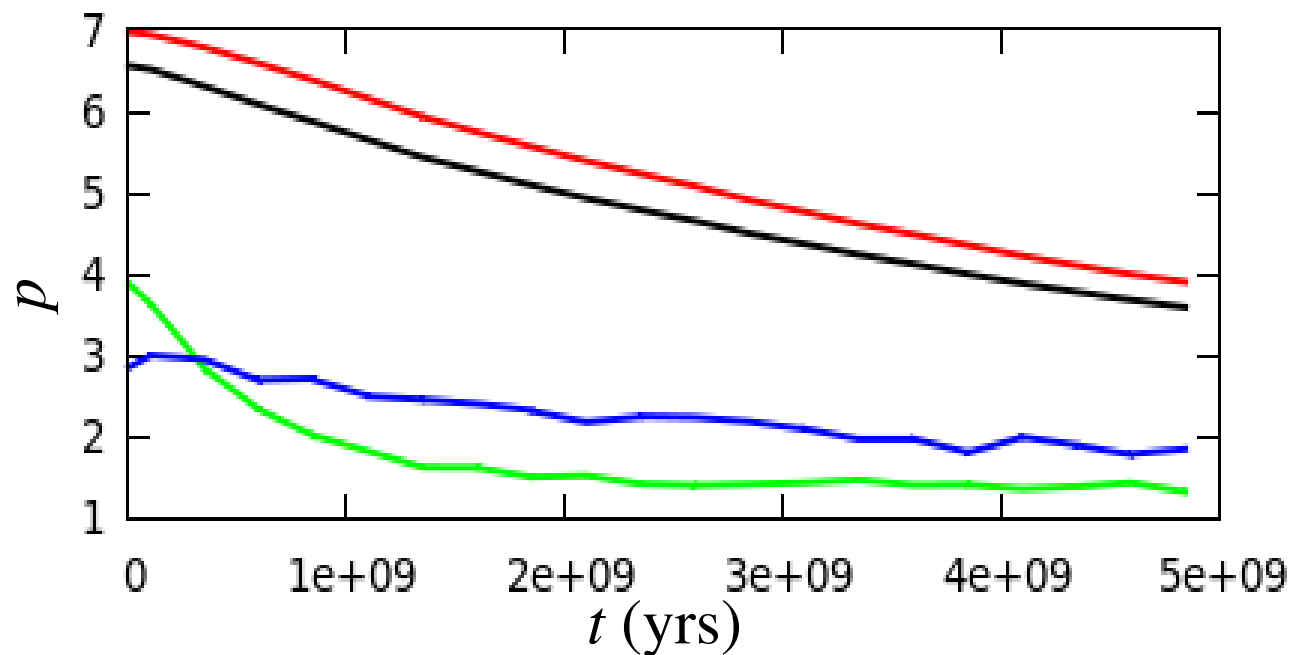
$$q_{\min} = a(1 - e_{\min}) \quad \text{with} \quad e_{\min} = f(e, \omega_G, i_G)$$

# Population in the Tidal Active Zone in the case of an initial thermalized population

We consider the percentage of comet in the Tidal Active Zone given by:

$$p = N_{\text{TAZ}} / N_{\text{Oort}} \times 100$$

- $a < 20\,000$  A.U. :  $p_{\text{max}} = 6.98 \%$
- $20\,000 < a < 50\,000$  A.U. :  $p_{\text{max}} = 3.88 \%$
- $a > 50\,000$  A.U. and  $a < 0$  :  $p_{\text{max}} = 2.84 \%$
- All :  $p_{\text{max}} = 6.56 \%$



# The action of stars

**The Oort cloud**

T.A.Z.  
 $q_{\min} < 5 \text{ A.U.}$

**The Oort cloud**

T.A.Z.  
 $q_{\min} < 5 \text{ A.U.}$

**The Oort cloud**

T.A.Z.  
 $q_{\min} < 5 \text{ A.U.}$

$$\tau_i = \frac{p(t^* - \epsilon)}{p_{\max}} \times 100$$

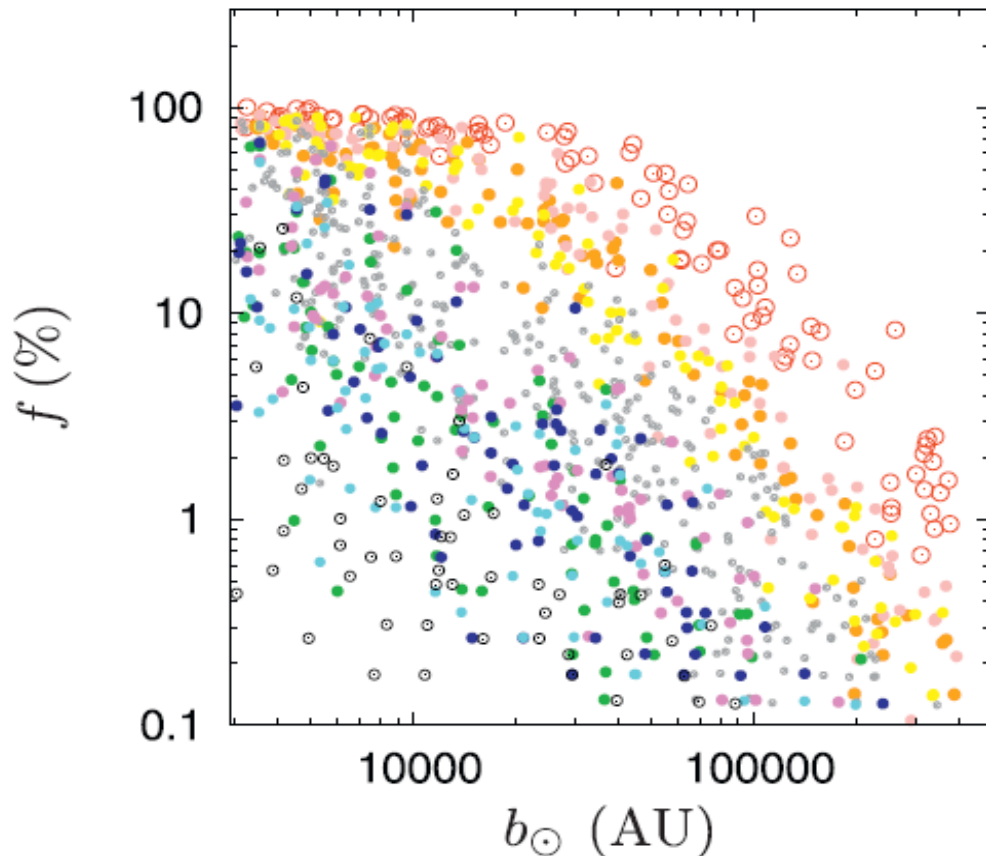
$$\tau_f = \frac{p(t^* + \epsilon)}{p_{\max}} \times 100$$



# Feeding of the Tidal Active Zone vs stellar parameters

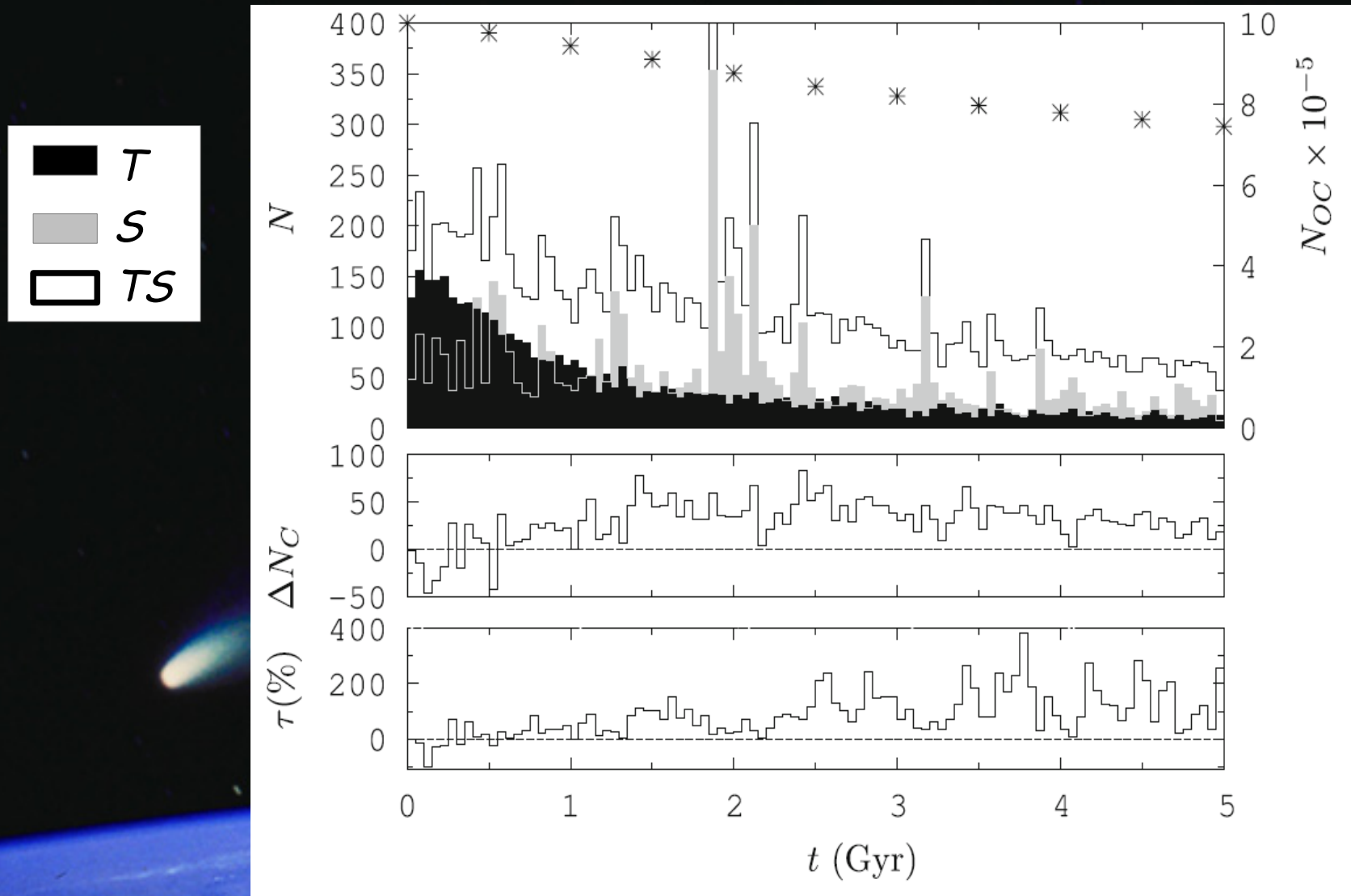
◻ : B0 (9  $M_{\odot}$ ), ● : gi (4  $M_{\odot}$ )    ● : A0 (1.2  $M_{\odot}$ ), ● : A5 (2.1  $M_{\odot}$ )  
● : F0 (1.7  $M_{\odot}$ ), F5 (1.3  $M_{\odot}$ ), G0 (1.1  $M_{\odot}$ ), G5 (0.93  $M_{\odot}$ )  
● : K0 (0.78  $M_{\odot}$ ), ● : wd (0.9  $M_{\odot}$ )    ● : K5 (0.69  $M_{\odot}$ )    ● : M0 (0.47  $M_{\odot}$ ), ○ : M5 (0.21  $M_{\odot}$ )

Central Oort cloud



Massive stars are able to fill completely the TAZ with much higher impact parameter than low mass stars

# The long term synergy



After 2 Gyr there is a strong synergy between the tides and stellar perturbations

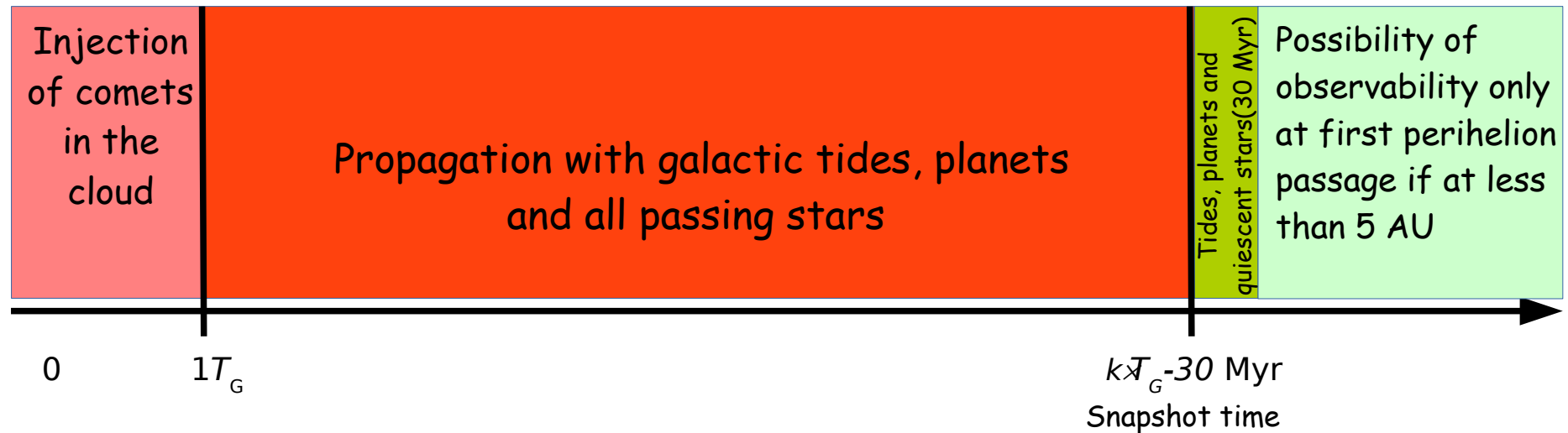
# Initial conditions and simulations

## Initial conditions:

$10^7$  comets randomly chosen with the following uniform distributions:

- perihelion distance  $q$  between 15 and 32 AU
- ecliptical inclination  $i$  between  $0^\circ$  and  $20^\circ$
- orbital energy for semi-major axis  $a$  between 1,100 and 50,000 AU
- uniform distribution of  $M, \omega$  and  $\Omega$  between  $0^\circ$  and  $360^\circ$ .

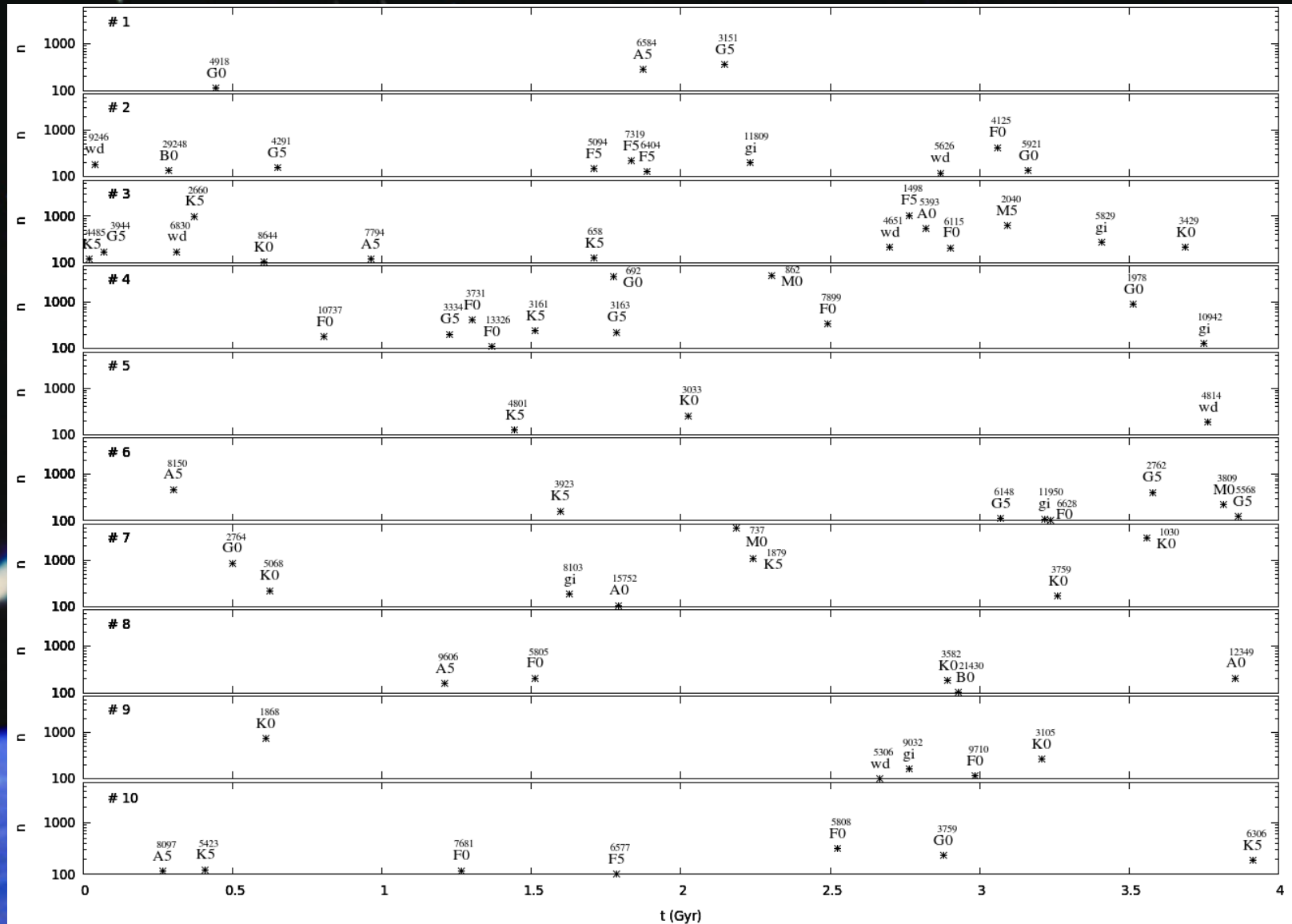
## Propagation:



NB:  $T_G$  is the orbital period of the Sun around the galactic centre ( $1T_G \approx 236 \text{ Myr}$ )

5 different snapshots of the Oort cloud between 4.02 and 4.96 Gyr  $\Rightarrow$  as if we had modelled the evolution of  $5 \times 10^7$  comets.

# The 10 stellar sequences





# Global strength of the stellar sequences

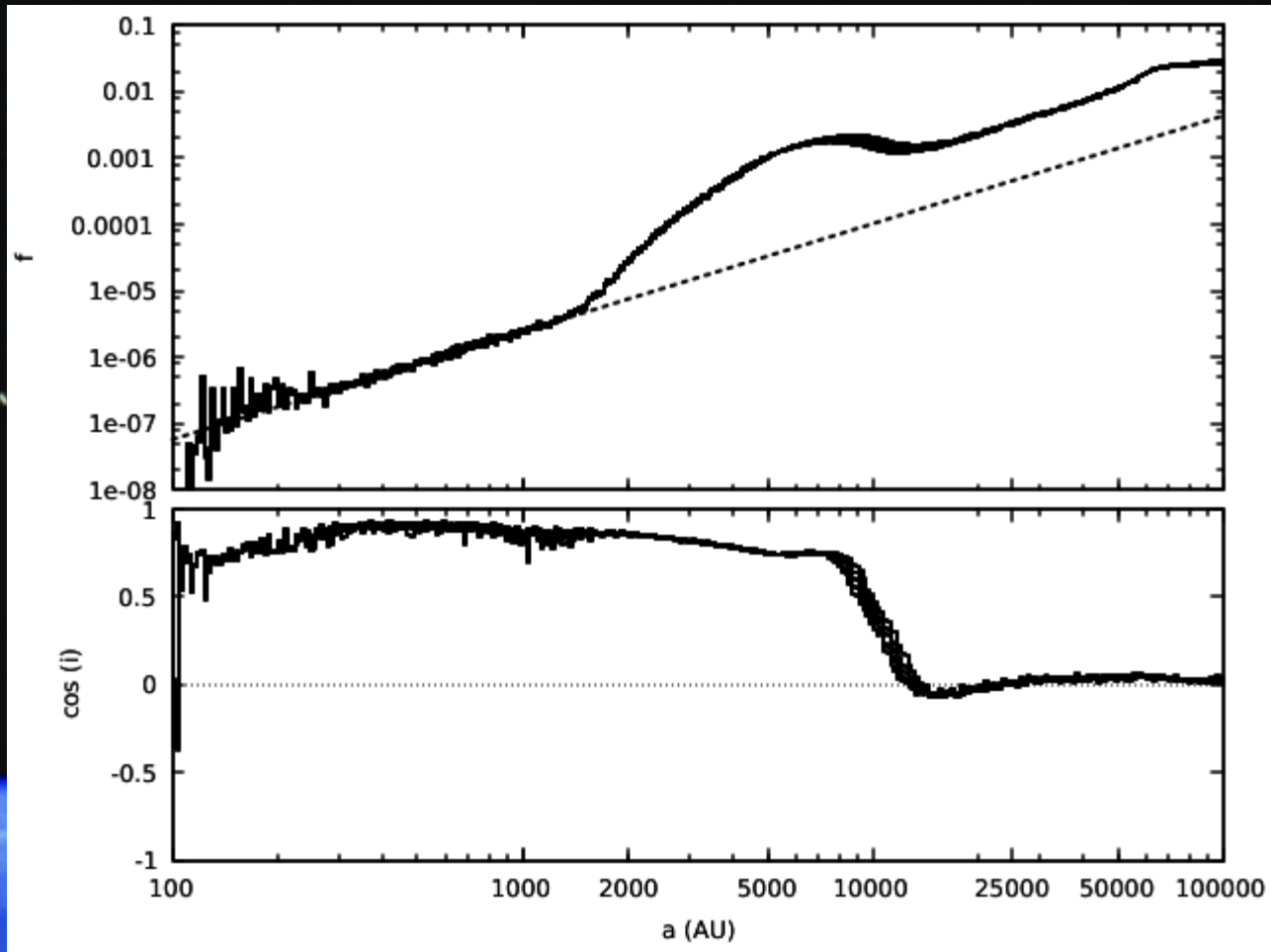
seq. #	$\Sigma_{N_{\star} > 10} N_{\star}$	Num. of stars with $N_{\star} >$		
		10	100	500
1	4001.1	142	3	0
2	4612.4	123	10	0
3	8127.5	139	14	4
4	12549.9	129	11	3
5	3917.6	132	3	0
6	4543.4	133	8	0
7	13490.3	140	8	4
8	3562.8	128	5	0
9	4538.7	138	5	1
10	4044.9	130	7	0

The estimated number of observable comets  $N_{\star}$  is given by a power law fit of the number of comets obtained numerically that are injected into the observable region from the Oort cloud by a single stellar passage.

# The final shape, without stellar perturbations - I

Five different snapshot times between 4 Gyr and 5 Gyr :

- The distributions overlap
- Two regimes:
  - below  $\approx 1,500$  AU a diffusive regime caused by planetary perturbations
  - beyond  $\approx 1,500$  AU, distribution shaped by the interaction between galactic tides and planetary perturbations.



# Some properties of the Galactic tides

The period of the perihelion is directly obtained from the orbital parameters and is inversely proportional to the orbital period :

$$P_p = \frac{1}{P_{\text{orb}}} f(e, i_G, \omega_G)$$

For each comet, we will consider the number of perihelion cycle during  $\Delta t$  :

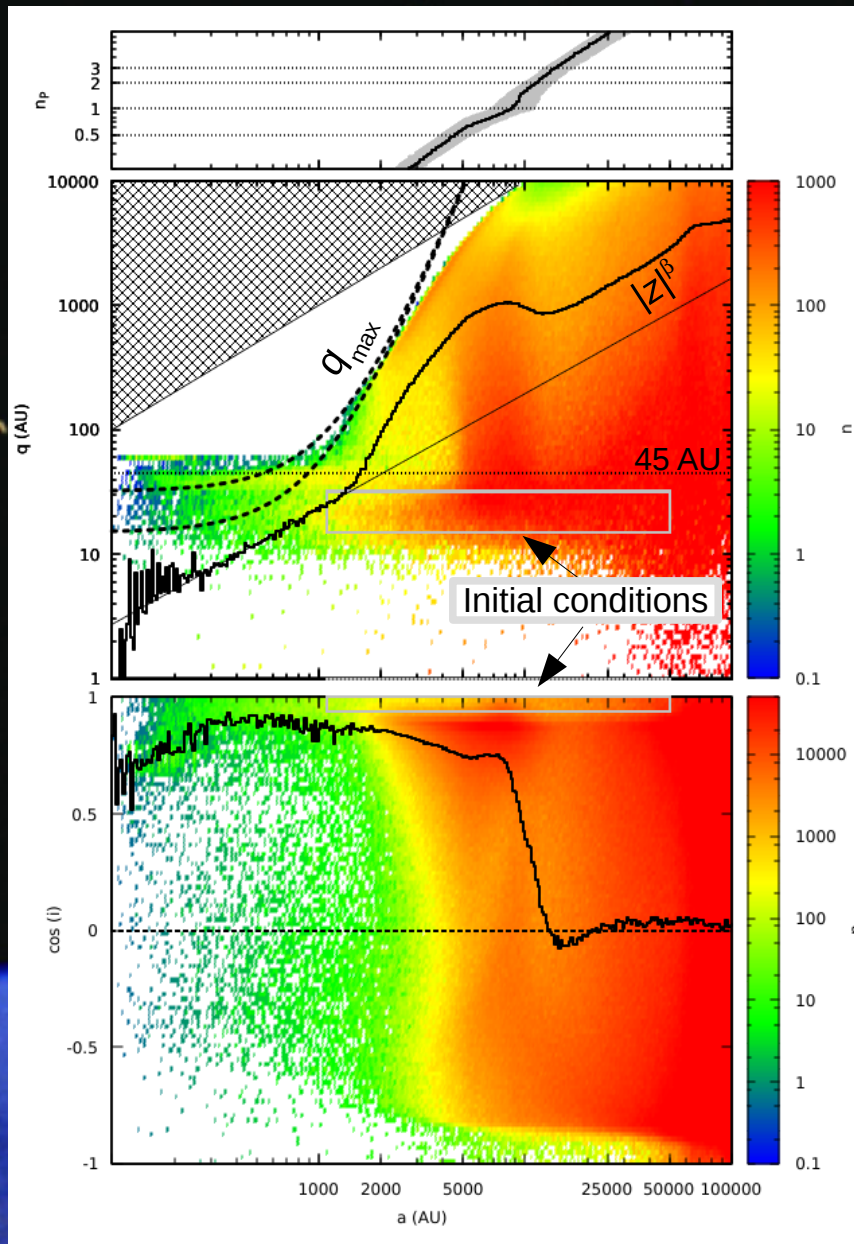
$$n_p = \frac{\Delta t}{P_e}$$

If  $\Delta t \ll P_e$  and  $e \approx 1$ , one can estimate the maximal and the median value of the perihelion distance that a comet can reach starting from  $q_0$  according to its semi-major axis :

$$q_{\text{max}} = \left( \sqrt{q_0} + \frac{5\sqrt{2} G_3}{8\mu} a^2 \Delta t \right)^2 \quad q_{\text{med}} = \left( \sqrt{q_0} + \frac{5\sqrt{2} G_3}{24\mu} a^2 \Delta t \right)^2$$



# The Final shape without stellar perturbations - II



The knee at about 1,500 AU is well explained by the  $q_{max}$  behaviours : it occurs when the tides are able to remove the perihelion from the planetary region in about 4.5 Gyr

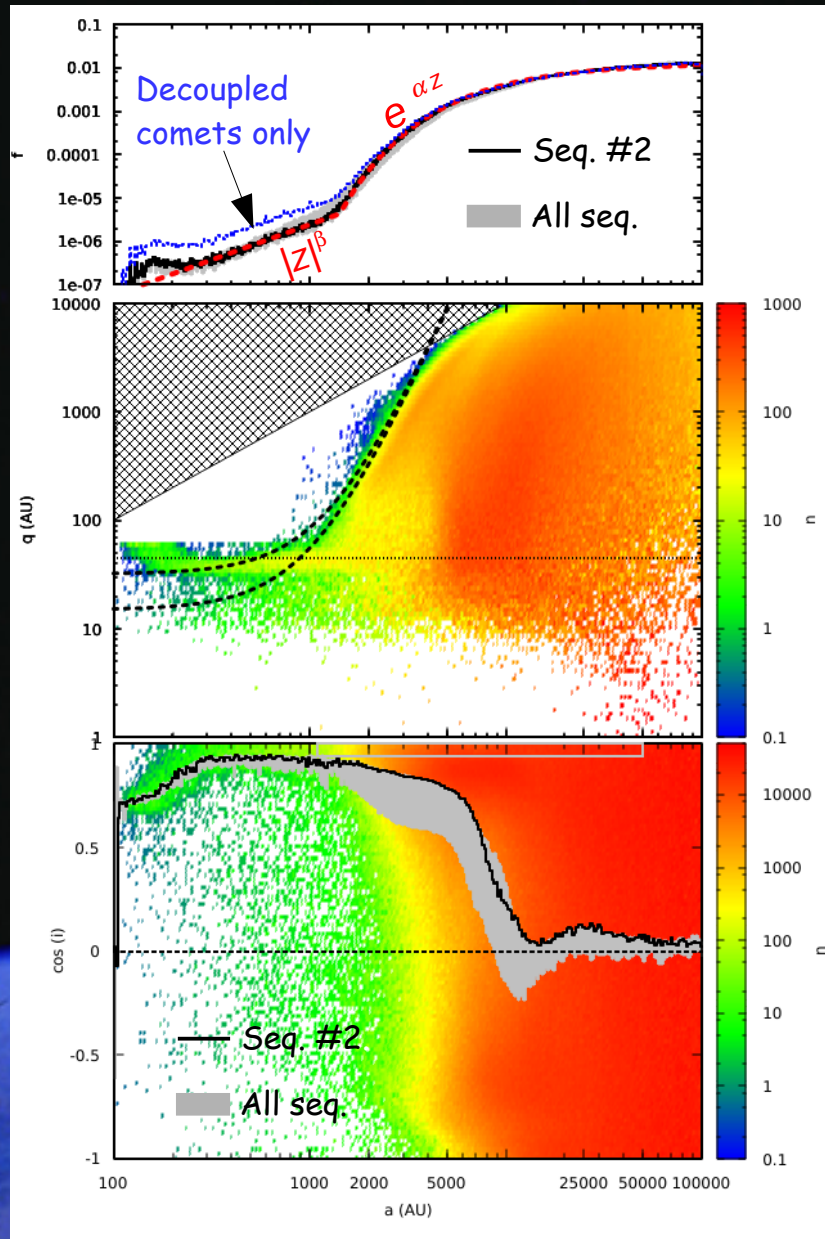
In the diffusive regime ( $a < 1,500$  AU) the orbital energy distribution is well approximated by a power law  $\mu |z|^\beta$ , with  $\beta = -1.62 \pm 0.3$

In the tidal region, the main features are:

- For  $2,300 < a < 6,500$  AU : an accumulation of comets at high perihelion distance corresponding to  $n_p \approx 0.5$
- For  $5,000 < a < 10,000$  AU : the perihelion distances are on their decreasing branch leading back to the planetary region. For  $7,000 < a < 11,000$  AU,  $n_p \approx 1$  meaning that most of the comets have performed a complete cycle  $\Rightarrow$  depletion of the Oort cloud caused by the planets. When  $a$  increases the time spent by the comets in the planetary region decreases given less chance to planetary ejection.
- The  $(\cos i, a)$  diagram highlights a wave structure well explained in Higuchi et al. (2007).



# The Final shape with stellar perturbations

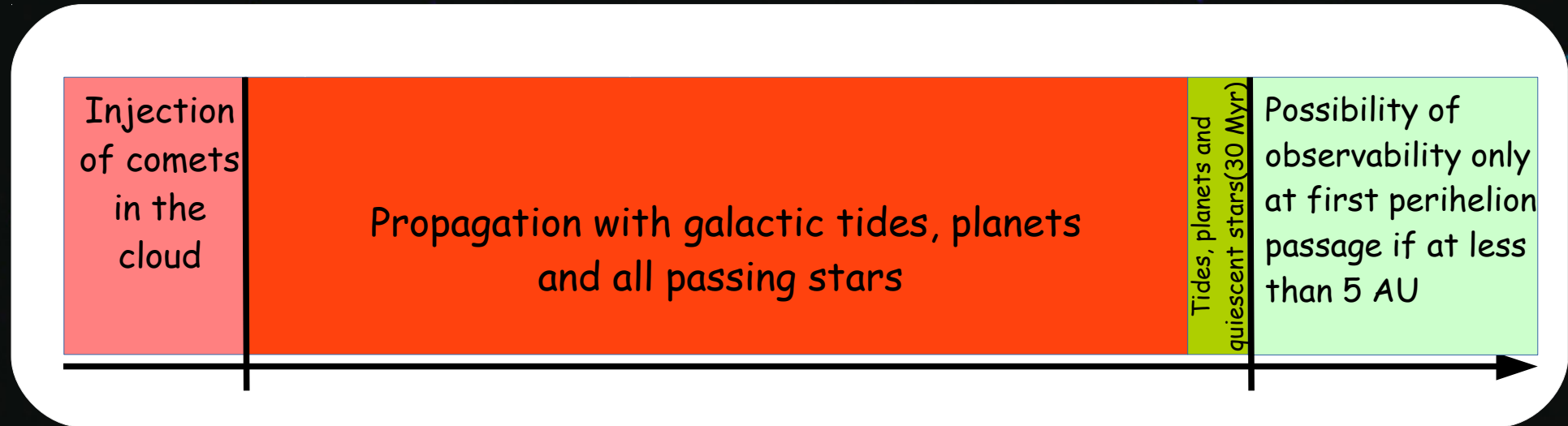


The final distributions of orbital energy has been smoothed in the tidal regime. Indeed, stellar perturbations have broken the tidal perihelion cycle.

This distribution is very robust with the knee between the diffusive and the tidal regime located between 1,000 and 2,000 AU. The tidal regime yield a Boltzmann distribution of orbital energy  $\mu e^{\alpha z}$ , with  $\alpha$  between 11,000 and 13,000 according to the stellar seq. Even considering only comets with  $a < 1,000$  AU at some time during the propagation (decoupled comets) the orbital energy distribution conserved the same properties.

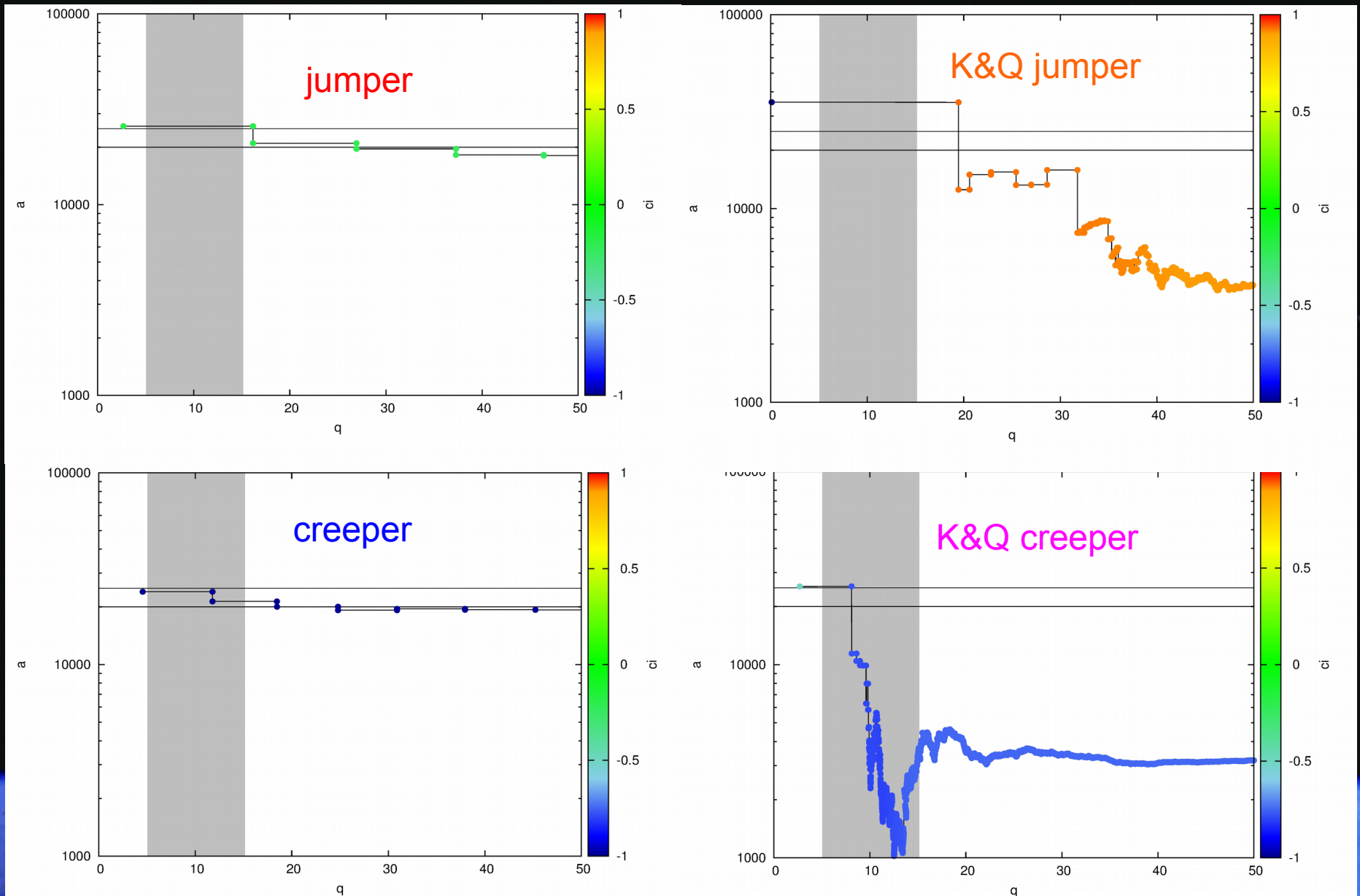
The behaviour of the median of  $\cos i$  is more dependent on the stel. seq. as explained in Higuchi and Kokubo (2015). However, whatever is the seq. the cloud is certainly not isotropic for  $a < 9,000$  AU.

# The observable comets



Each observable comet is weighted by :  $2 \times 10^4 / P_{\text{orb}}$   
so that it corresponds to an observable comet per  
year considering an initial Oort cloud containing  
 $10^{12}$  comets (Kaib and Quinn 2009, Brasser and Mordbidelli 2013).

# The four observable classes



KQ stands for Kaib and Quinn (2009)



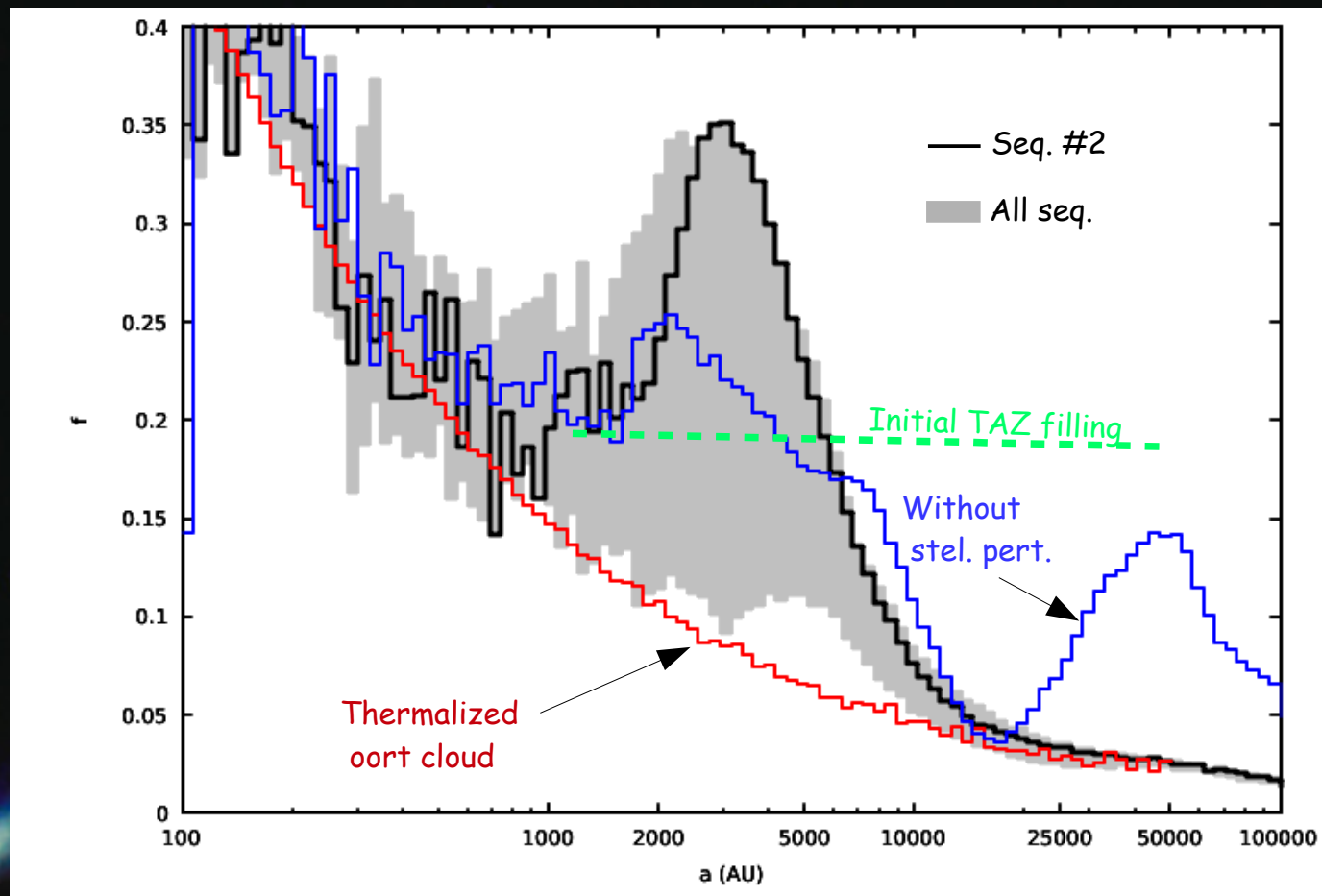
# Global statistics on the observable comets

mod.	c/yr	j	c	KQ j	KQ c	$a_{050}$	ret.	$a_{\text{orig}_{25}}$	$a_{\text{orig}_{50}}$
1	4.5	44.9	17.4	1.2	36.5	2412.3	53.3	21092.6	28081.4
2	4.5	41.4	17.8	1.3	39.6	2497.9	49.9	22097.9	28157.0
3	3.3	41.4	17.6	1.1	39.9	2208.5	56.5	21198.6	27828.0
4	3.3	39.8	17.3	0.9	42.1	2230.3	55.0	21837.1	27445.2
5	5.1	40.2	19.2	0.4	40.2	2253.6	54.4	20623.0	27256.7
6	3.9	44.7	16.4	1.3	37.7	2431.9	51.8	22189.7	28562.6
7	3.2	41.8	16.4	1.2	40.5	2343.6	57.6	20120.4	26963.0
8	4.0	43.6	19.1	0.8	36.4	2395.9	57.6	21501.7	28634.6
9	4.4	42.3	18.7	0.7	38.3	2519.9	55.7	22044.8	28458.8
10	5.3	44.1	19.4	0.9	35.6	2328.4	55.4	21400.6	27801.9
TP	8.2	69.8	14.1	2.4	13.6	2266.8	50.6	29660.7	41470.6

- The production of comets with a total magnitude  $H_T < 11$  is consistent with Francis (2005) and Brassier and Morbidelli (2013).
- When stellar perturbations are at work, a majority of comets were in the Jupiter-Saturn barrier at their previous perihelion passage, and the median and the first quartile of the observable comets original semi-major axis have been reduced.
- In almost all cases a small preference for retrograde orbits seems to be observed.



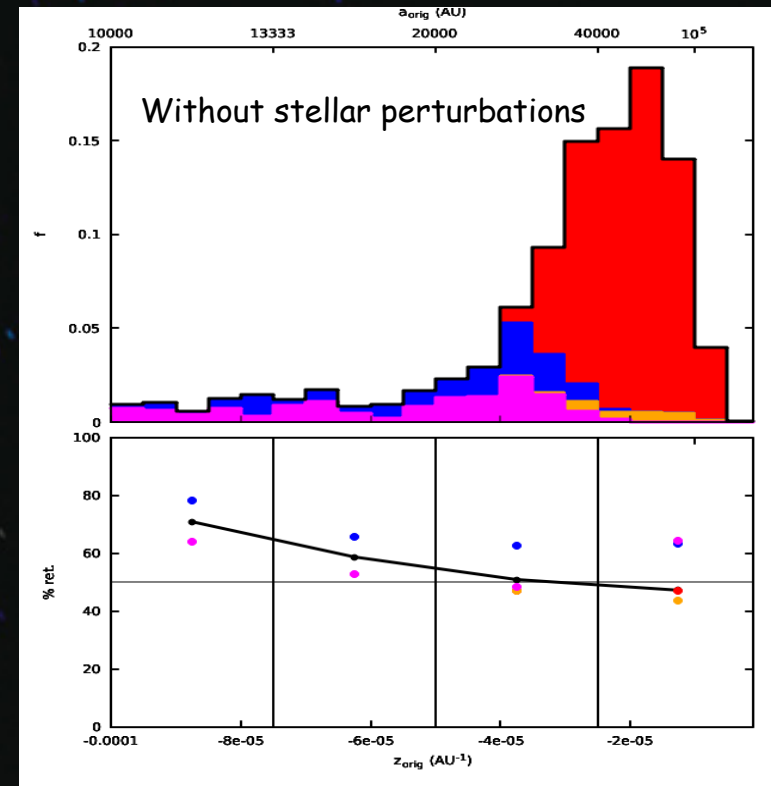
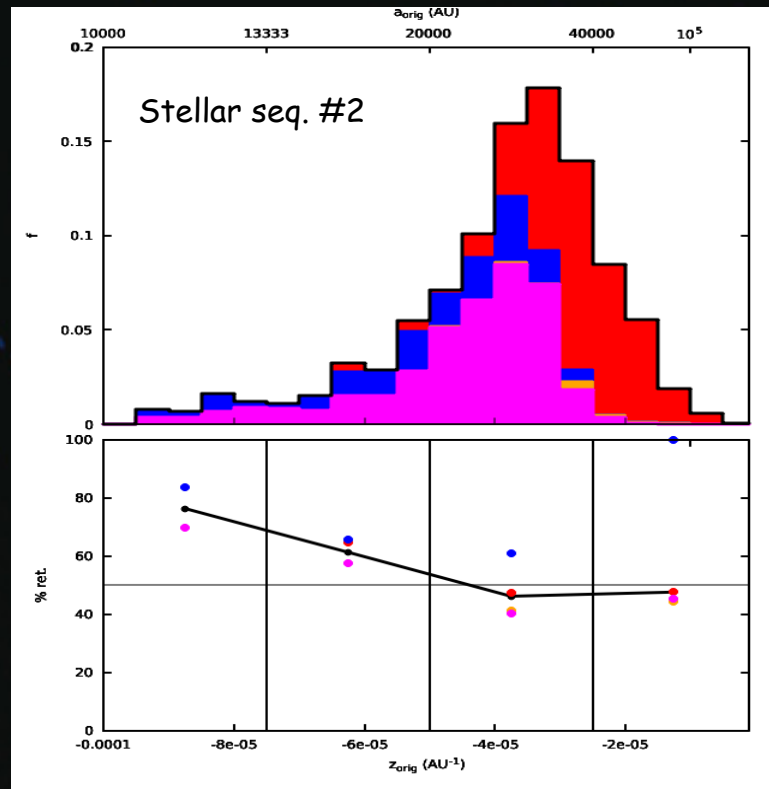
# The final TAZ filling



Convergence toward the thermalized cloud for  $a < 1,000$  AU (planetary perturbations) and  $a > 10,000$  AU (stellar perturbations).

Without star the departure from the initial filling for  $a > 5,000$  AU is caused by the depletion of the TAZ by planetary perturbations. This depletion is less efficient for increasing semi-major axis because of the fast transit of the perihelion through the planetary region.

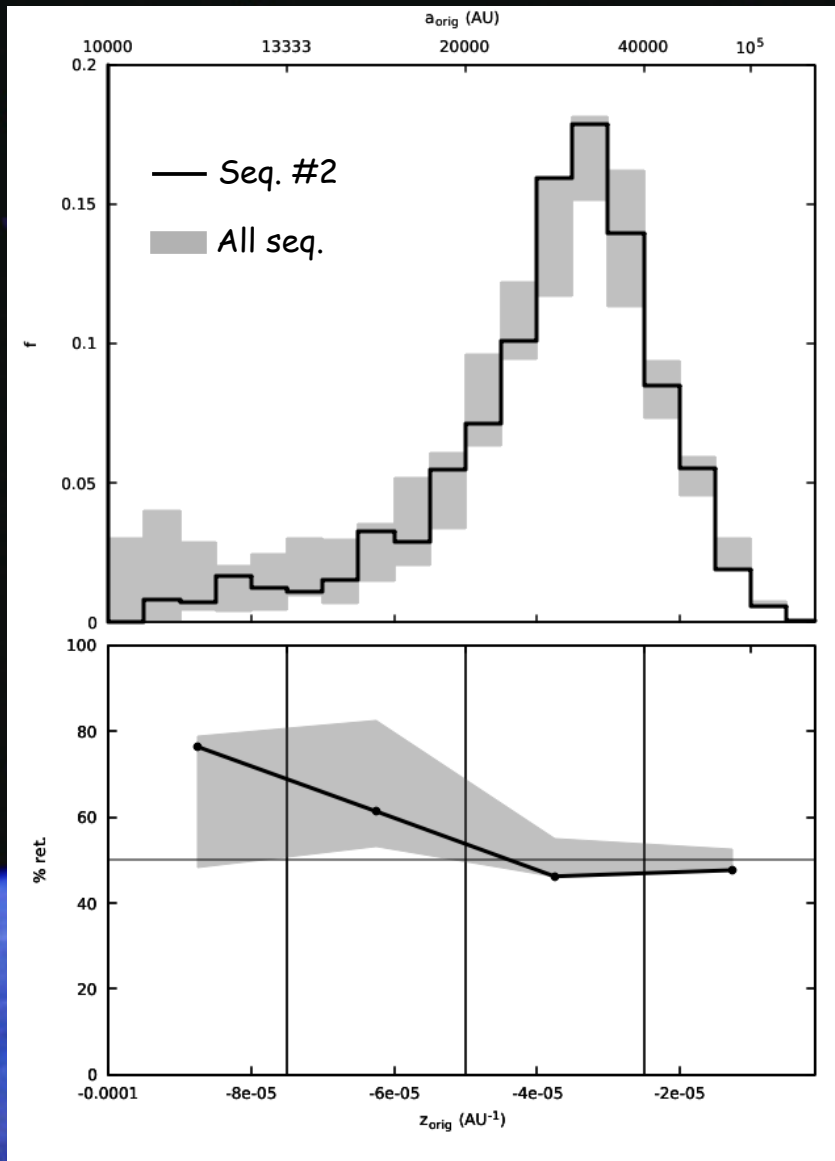
# The Oort spike



The spike is shift to smaller semi-major axis when stellar perturbations are at work. The preference is for creepers and KQ creepers, whereas without stellar perturbations observable comets are clearly jumpers for their majority. This is explainable by the TAZ filling : creepers and KQ creepers are coming from smaller semi-major axis ( $< 20,000$  AU, Fouchard et al. 2014) where the TAZ is more filled when stellar perturbations are at work, whereas the jumpers come mainly for a  $> 25,000$  AU, where the TAZ is more filled when the stars are not at work.

As regard the proportion of retrograde orbits, a preference for retrograde orbits is observed when creepers and KQ creepers dominate. 22

# Oort spike : other stellar sequences

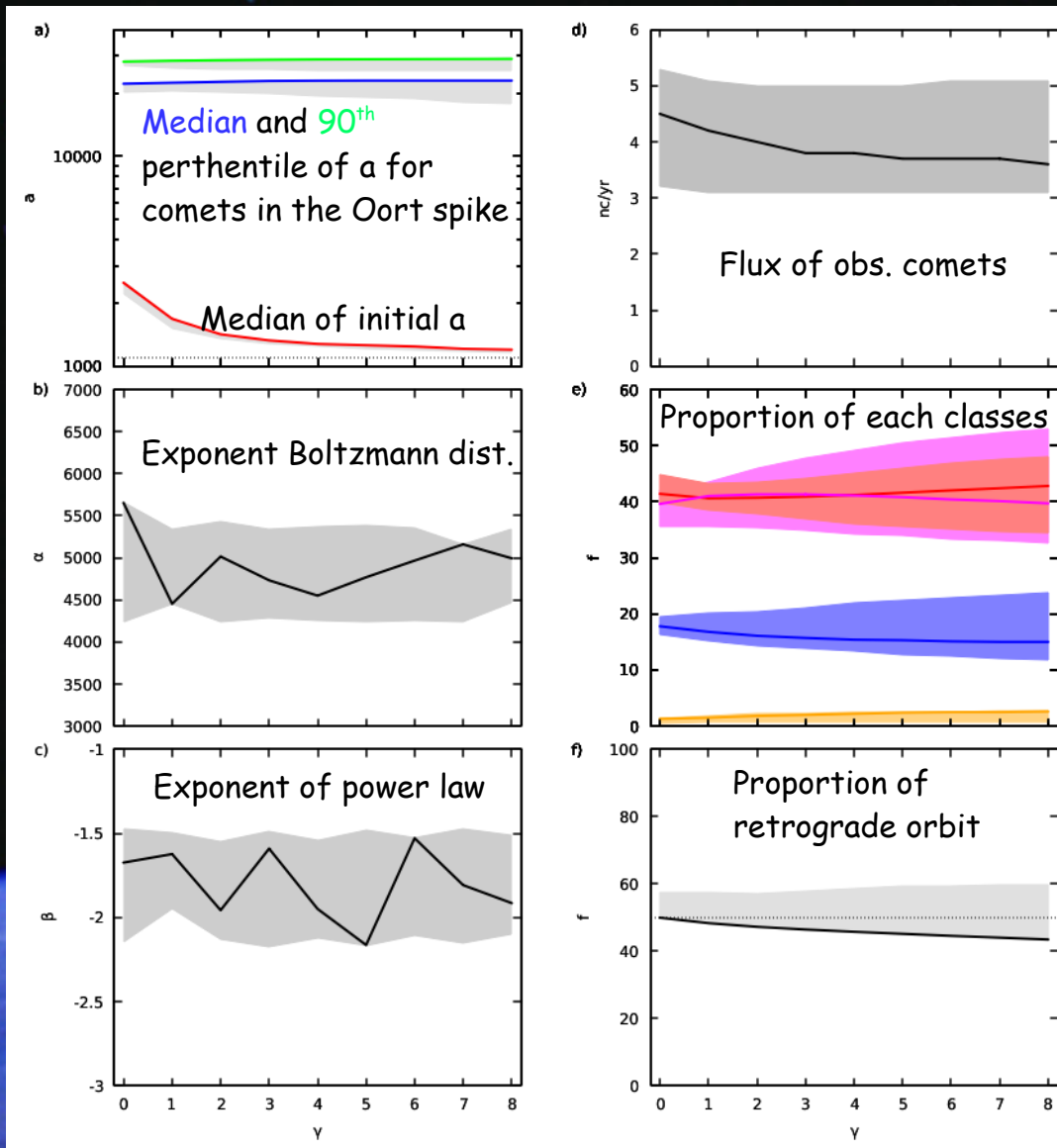


The shape of the spike is rather robust with respect to the stellar sequence used.

The proportion of retrograde orbits is on the contrary very sensitive to the stellar sequence, mainly for  $a < 20,000$  AU. This is mainly caused by statistical fluctuations because of the small number of observable comets.



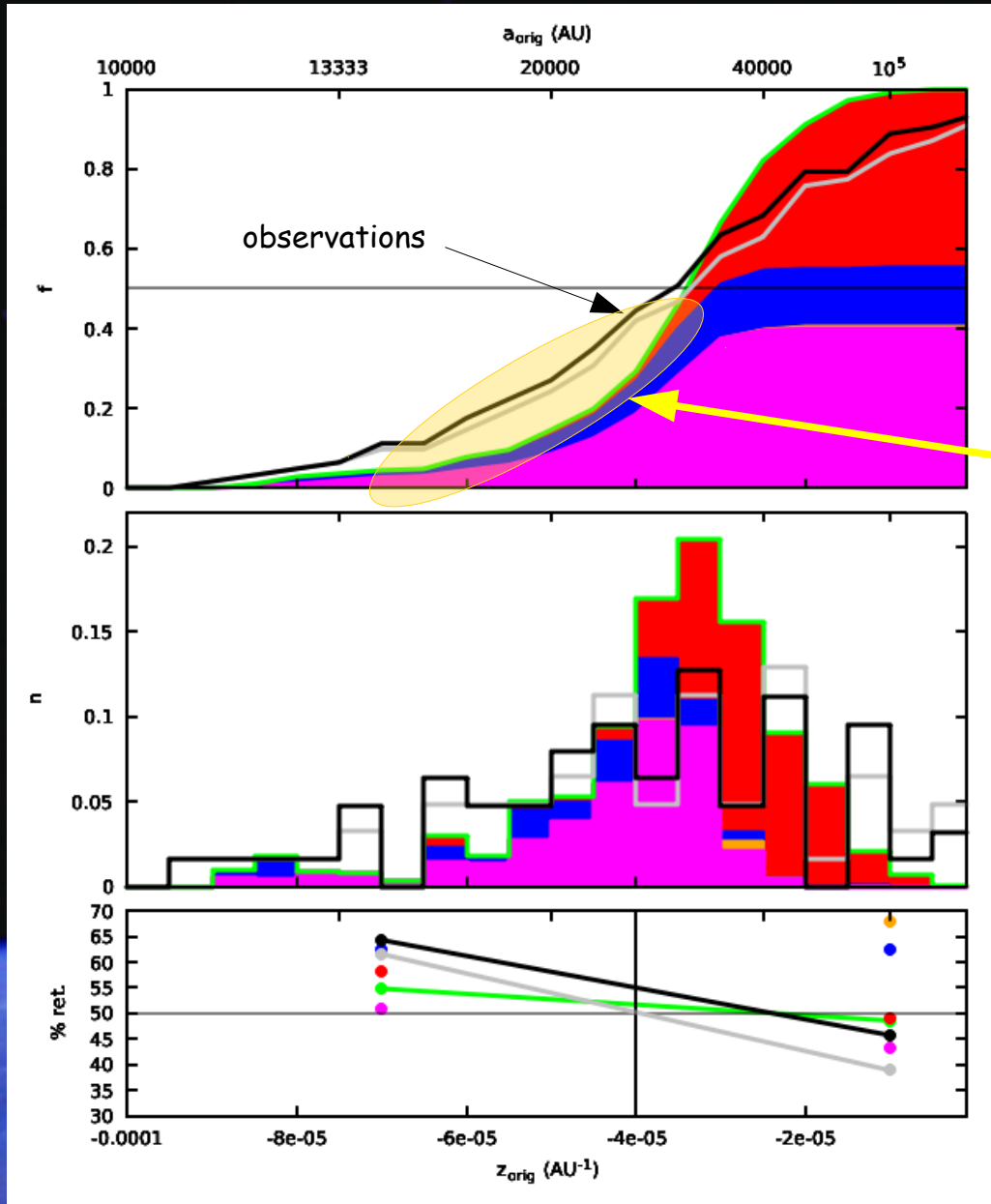
# Influence of the initial orbital distributions



The original orbital energy distribution is uniform. We simulate distributions proportional to  $z^\gamma$  by applying a weight ( $\mu z_o^{\gamma-1}$ ) to the comet according to their initial orbital energy  $z_o$ .



# Comparison with observations



Discrepancy. Caused by :

- Planet nine ?
- Higher stellar density of low mass stars in the solar neighbourhood ?
- Wrong determination of the original orbital energy ?



*Thank you*